

Properties of proto neutron star PSR J0737-3039A*

Xian-Feng Zhao(赵先锋)[†] Shui-Rong Zhong(钟水蓉) Jian-Li Huo(霍建立)

School of Sciences, Southwest Petroleum University, Chengdu 610500, China

Abstract: Using five sets of nucleon coupling constants (DD-ME1, GL85, GL97, GM1, and NL2), we find that the radius of the PNS PSR J0737-3039A is $R=15.693-18.846$ km, the central baryon density is $\rho_c=0.247-0.359$ fm⁻³, the central energy density is $\varepsilon_c=4.30\times 10^{14}-6.49\times 10^{14}$ g·cm⁻³, and the central pressure is $p_c=3.79\times 10^{34}-5.85\times 10^{34}$ dyne·cm⁻². With DD-ME1, GL85, GL97, and GM1, baryon octets appear in the PNS PSR J0737-3039A. With NL2, only the baryons $n, p, \Lambda, \Sigma^0, \Sigma^-, \Xi^0$, and Ξ^- are present. Corresponding to the same baryon density, the relative densities of the same baryon in the PNS PSR J0737-3039A calculated using different nucleon coupling constants differ greatly. The central relative baryon densities of the PNS PSR J0737-3039A calculated using different nucleon coupling constants also differ greatly.

Keywords: baryon, relativistic mean field theory, proto neutron star

DOI: 10.1088/1674-1137/ac76a6

I. INTRODUCTION

The 2.8-second pulsar J0737-3039B is the companion of the 23-millisecond pulsar J0737-3039A. The two pulsars form a highly relativistic binary neutron star (NS) system [1], and the mass of the NS J0737-3039A should be related to the mass and metallicity of its companion [2]. The NS J0737-3039A has a mass $M=1.34 M_\odot$, which is typical for NSs [1, 3, 4].

Morrison *et al.* constructed a numerical model of the binary pulsar J0737-3039A using its measured mass, spin, and moment of inertia to determine the optimal model for different equations of state (EoS) so as to determine the radius of the pulsar. The NS they used, PSR J0737-3039A, has a gravitational mass $M=1.337 M_\odot$ [5]. In 2006, Kramer *et al.* more accurately determined the mass of the NS PSR J0737-3039A to be $M = 1.3381\pm 0.0007 M_\odot$ [6].

In 2008, Worley *et al.* placed special emphasis on the PSR J0737-3039A component of the extremely relativistic double NS system PSR J0737-3039. They found its moment of inertia to be between 1.30×10^{45} g·cm² and 1.63×10^{45} g·cm² [7]. Using well-known universal relations between NS observables, Landry *et al.* translated the reported 90%-credible bounds on tidal deformability into a direct constraint on the moment of inertia of PSR J0737-3039A [8].

In 2020, Avdeev *et al.* developed a parameterized

post-Keplerian formalism for hybrid metric-Palatini $f(R)$ -gravity and obtained the mass ratio $M_A/M_B=1.0714$. On this basis, they predicted the mass of the NS PSR J0737-3039A as $1.3374 M_\odot < M < 1.3440 M_\odot$ in the framework of hybrid $f(R)$ -gravity [9].

An NS has a high density, strong magnetic field, and high rotation speed [10–16]. Several massive NSs, PSR J1614-2230 [17, 18], PSRJ0348+0432 [19], and PSRJ0740+6620 [20], have been observed in recent years. Although the NS PSR J0737-3039A has a significantly smaller mass than these, its mass is typical, and it is a member of a binary NS system. Therefore, theoretical research on this NS is important.

NSs are formed by the neutrino radiation cooling of proto neutron stars (PNSs) [21]. Studying PNSs is vital for understanding the evolution of stars. Therefore, we are very interested in the PNS PSR J0737-3039A.

In this study, we investigate the properties of the PNS PSR J0737-3039A with relativistic mean field (RMF) theory [22] considering a baryon octet.

II. RMF THEORY OF PNS MATTER

The mesons $f_0(975)$ (denoted as σ^*) and $\phi(1020)$ (denoted as ϕ) represent the interactions between nucleons and hyperons [23]. The Lagrangian density of hadronic matter containing the mesons σ^* and ϕ is expressed as follows [24]:

Received 30 April 2022; Accepted 8 June 2022; Published online 29 July 2022

* Supported by the Natural Science Foundation of China (11447003) and the Special Project of Science and Technology Strategic Cooperation between Nanchong City and Southwest Petroleum University (SXHZ017)

[†] E-mail: zhaopioneer.student@sina.com

©2022 Chinese Physical Society and the Institute of High Energy Physics of the Chinese Academy of Sciences and the Institute of Modern Physics of the Chinese Academy of Sciences and IOP Publishing Ltd

$$\begin{aligned} \mathcal{L} = & \sum_B \bar{\Psi}_B (i\gamma_\mu \partial^\mu - m_B + g_{\sigma B} \sigma + g_{\sigma^* B} \sigma^* \\ & - g_{\omega B} \gamma^0 \omega - g_{\phi B} \gamma^0 \phi - g_{\rho B} \gamma^0 \tau_3 \rho) \Psi_B \\ & - \frac{1}{2} m_\sigma^2 \sigma^2 - \frac{1}{3} g_2 \sigma^3 - \frac{1}{4} g_3 \sigma^4 \\ & + \frac{1}{2} m_\omega^2 \omega^2 + \frac{1}{2} m_\rho^2 \rho^2 - \frac{1}{2} m_{\sigma^*}^2 \sigma^{*2} + \frac{1}{2} m_\phi^2 \phi^2 \\ & + \sum_{\lambda=e,\mu} \bar{\Psi}_\lambda (i\gamma_\mu \partial^\mu - m_\lambda) \Psi_\lambda. \end{aligned} \quad (1)$$

Considering neutrino binding, the baryon partition function of PNS matter is [25, 26]

$$\ln Z_B = \frac{V}{T} \langle \mathcal{L} \rangle + \sum_B \frac{2J_B + 1}{2\pi^2} \int_0^\infty k^2 dk \left\{ \ln \left[1 + e^{-(\varepsilon_B(k) - \mu_B)/T} \right] \right\}. \quad (2)$$

From the above, the total baryon number density is obtained as follows:

$$\rho = \sum_B \frac{2J_B + 1}{2\pi^2} b_B \int_0^\infty k^2 n_B(k) dk. \quad (3)$$

The energy density and pressure are respectively

$$\begin{aligned} \varepsilon = & \frac{1}{2} m_\sigma^2 \sigma^2 + \frac{1}{2} m_{\sigma^*}^2 \sigma^{*2} + \frac{1}{3} g_2 \sigma^3 \\ & + \frac{1}{4} g_3 \sigma^4 + \frac{1}{2} m_\omega^2 \omega_0^2 + \frac{1}{2} m_\phi^2 \phi^2 + \frac{1}{2} m_\rho^2 \rho_{03}^2 \\ & + \sum_B \frac{2J_B + 1}{2\pi^2} \int_0^\infty k^2 n_B(k) dk \sqrt{k^2 + m_B^{*2}}, \end{aligned} \quad (4)$$

$$\begin{aligned} p = & -\frac{1}{2} m_\sigma^2 \sigma^2 - \frac{1}{2} m_{\sigma^*}^2 \sigma^{*2} - \frac{1}{3} g_2 \sigma^3 \\ & - \frac{1}{4} g_3 \sigma^4 + \frac{1}{2} m_\omega^2 \omega_0^2 + \frac{1}{2} m_\phi^2 \phi^2 + \frac{1}{2} m_\rho^2 \rho_{03}^2 \\ & + \frac{1}{3} \sum_B \frac{2J_B + 1}{2\pi^2} \int_0^\infty \frac{k^4}{\sqrt{k^2 + m_B^{*2}}} n_B(k) dk. \end{aligned} \quad (5)$$

Here, $n_B(k)$ is the Fermi-Dirac partition function of baryons,

$$n_B(k) = \frac{1}{1 + \exp[(\varepsilon_B(k) - \mu_B)/T]}, \quad (6)$$

and m_B^* is the effective mass of baryons,

$$m_B^* = m_B - g_{\sigma B} \sigma - g_{\sigma^* B} \sigma^*. \quad (7)$$

Ignoring the interactions of leptons at finite temperature, we express their partition function as

$$\begin{aligned} \ln Z_L = & \frac{V}{T} \sum_i \frac{\mu_i^4}{24\pi^2} \left[1 + 2 \left(\frac{\pi T}{\mu_i} \right)^2 + \frac{7}{15} \left(\frac{\pi T}{\mu_i} \right)^4 \right] \\ & + V \sum_\lambda \frac{1}{\pi^2} \int_0^\infty k^2 dk \left\{ \ln \left[1 + e^{-(\varepsilon_\lambda(k) - \mu_\lambda)/T} \right] \right\}, \end{aligned} \quad (8)$$

where the first line represents the contribution of massless neutrinos, and the second line represents the contribution of electrons and μ s.

The lepton number density is

$$\rho_l = \frac{1}{\pi^2} \int_0^\infty k^2 n_l(k) dk, \quad (9)$$

$$\rho_\nu = \frac{\pi^2 T^2 \mu_\nu + \mu_\nu^3}{6\pi^2} \quad (10)$$

and the contributions of leptons to the energy density and pressure are respectively

$$\begin{aligned} \varepsilon = & \sum_l \frac{1}{\pi^2} \int_0^\infty k^2 n_l(k) dk \sqrt{k^2 + m_l^2} \\ & + \sum_\nu \left(\frac{7\pi^2 T^4}{120} + \frac{T^2 \mu_\nu^2}{4} + \frac{\mu_\nu^4}{8\pi^2} \right), \end{aligned} \quad (11)$$

$$\begin{aligned} p = & \frac{1}{3} \sum_l \frac{1}{\pi^2} \int_0^\infty \frac{k^4}{\sqrt{k^2 + m_l^2}} n_l(k) dk \\ & + \sum_\nu \frac{1}{360} \left(7\pi^2 T^4 + 30T^2 \mu_\nu^2 + \frac{15\mu_\nu^4}{\pi^2} \right). \end{aligned} \quad (12)$$

The chemical potentials of baryons are

$$\mu_i = \mu_n - q_i (\mu_e - \mu_\nu). \quad (13)$$

To describe neutrino trapping, the content of leptons in a PNS is defined as

$$Y_{l\nu} = Y_l + Y_{\nu l} = \frac{\rho_l + \rho_{\nu l}}{\rho}. \quad (14)$$

We can calculate the mass and radius of a PNS using the Tolman-Oppenheimer-Volkoff (TOV) equations [27, 28]

$$\frac{dp}{dr} = -\frac{(p + \varepsilon)(M + 4\pi r^3 p)}{r(r - 2M)}, \quad (15)$$

$$M = 4\pi \int_0^R \varepsilon r^2 dr. \quad (16)$$

III. PARAMETERS

Here, we calculate the parameters of the PNS PSR J0737-3039A with five sets of nucleon coupling constants (DD-ME1 [29], GL85 [30], GL97 [24], GM1 [31], and NL2 [32]). For the outer crust with $4.73 \times 10^{-15} < \rho < 8.907 \times 10^{-3} \text{ fm}^{-3}$, we use the EoS of a BPS [24], and for the region of $\rho > 8.907 \times 10^{-3} \text{ fm}^{-3}$, we use the EoS for PNS matter corresponding to the nuclear properties above.

The ratios of the hyperon coupling constant to nucleon coupling constant are defined as $x_{\sigma h} = g_{\sigma h}/g_{\sigma}$, $x_{\omega h} = g_{\omega h}/g_{\omega}$, and $x_{\rho h} = g_{\rho h}/g_{\rho}$, with h denoting the hyperons Λ, Σ , and Ξ .

$x_{\rho h}$ and $x_{\omega h}$ are chosen using $SU(6)$ symmetry [33, 34]. Then, $x_{\sigma h}$ is obtained using [24]

$$U_h^{(N)} = m_n \left(\frac{m_n^*}{m_n} - 1 \right) x_{\sigma h} + \left(\frac{g_{\omega}}{m_{\omega}} \right)^2 \rho_0 x_{\omega h}. \quad (17)$$

In this study, the hyperon-potentials are chosen as $U_{\Lambda}^{(N)} = -30 \text{ MeV}$ [34, 35, 36], $U_{\Sigma}^{(N)} = 30 \text{ MeV}$ [34, 35, 36, 37], and $U_{\Xi}^{(N)} = -14 \text{ MeV}$ [38].

The coupling constants of the mesons σ^* and ϕ can be chosen as [23]

$$g_{\phi\Xi} = 2g_{\phi\Lambda} = 2g_{\phi\Sigma} = -2\sqrt{2}g_{\omega}/3, \quad (18)$$

$$g_{\sigma^*\Lambda}/g_{\sigma} = g_{\sigma^*\Sigma}/g_{\sigma} = 0.69, \quad (19)$$

$$g_{\sigma^*\Xi}/g_{\sigma} = 1.25. \quad (20)$$

Temperatures in the interiors of PNSs can reach up to 30 MeV. After that, they can be cooled by neutrino radiation [21]. In this study, the temperature of the PNS PSR J0737-3039A is taken as $T=20 \text{ MeV}$.

IV. RADIUS OF PNS PSR J0737-3039A

The mass M of the PNS is calculated as a function of the radius R . In Fig. 1, the coarse curves indicate the masses of the PNSs PSR J0740+6620, PSR J0348+0432, PSR J1614-2230, and PSR J0737-3039A, and the five fine curves represent the results of the five nucleon coupling constants DD-ME1, GL85, GL97, GM1, and NL2. We find that only the nucleon coupling constant DD-ME1 can give the masses of the PNSs PSR J0740+6620, PSR J0348+0432, PSR J1614-2230, and PSR J0737-3039A. NL2 cannot give the mass of the PNS PSR J0740+6620; however, it can give the mass of the PNSs PSR J0348+0432, PSR J1614-2230, and PSR J0737-3039A. GL85, GL97, and GM1 cannot give the masses of the PNSs PSR J0740+6620, PSR J0348+0432, and PSR

J1614-2230; however, they can give the masses of the PNS PSR J0737-3039A. All five sets of nucleon coupling constants give the masses of the PNS PSR J0737-3039A.

As shown in Fig. 1 and Table 1, the radii of the PNS PSR J0737-3039A given by the five sets of nucleon coupling constants are different. NL2 gives the smallest radius, $R=15.693 \text{ km}$, and GL85 gives the largest radius, $R=18.846 \text{ km}$. In other words, the radius of the PNS PSR J0737-3039A calculated using these five sets of nucleon coupling constants is $R=15.693\text{--}18.846 \text{ km}$. The NS PSR J0030+0451 has a mass similar to that of the PNS PSR J0737-3039A; hence, it is logical to compare their radii. The mass and radius of the NS PSR J0030+0451 given by Riley *et al.* are in the ranges $M=1.18\text{--}1.49 M_{\odot}$ and $R=11.52\text{--}13.85 \text{ km}$ [39], respectively, and those given by Miller *et al.* are $M=1.30\text{--}1.59 M_{\odot}$ and $R=11.96\text{--}14.26 \text{ km}$, respectively [40]. The PNS radius calculated in this study is larger than that calculated by Riley *et al.* and Miller *et al.*, which is reasonable because the radius of a

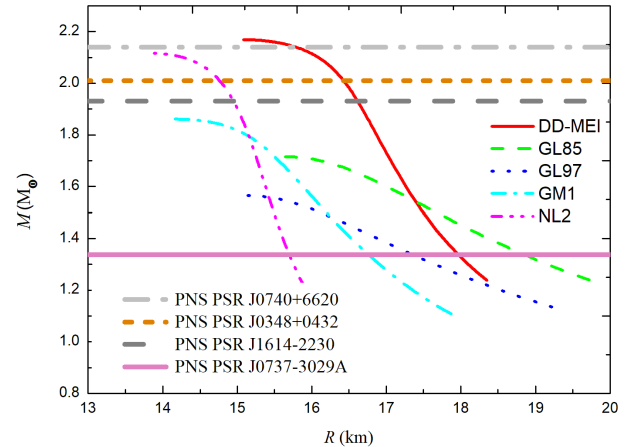


Fig. 1. (color online) Mass M of the PNS calculated as a function of the radius R . The coarse curves indicate the masses of the PNSs PSR J0740+6620, PSR J0348+0432, PSR J1614-2230, and PSR J0737-3039A. The five fine curves represent the results of the five nucleon coupling constants DD-ME1, GL85, GL97, GM1, and NL2.

Table 1. Results calculated in this study. The mass of the PNS PSR J0737-3039A is $M=1.338 M_{\odot}$. R , ρ_c , ε_c , and p_c are the radius, central baryon density, central energy density, and central pressure of the PNS PSR J0737-3039A, respectively.

Parameter	R/km	ρ_c/fm^{-3}	$\varepsilon_c \times 10^{15}/(\text{g} \cdot \text{cm})^{-3}$	$p_c \times 10^{35}/(\text{dyne} \cdot \text{cm})^{-2}$
DD-ME1	18.006	0.247	0.430	0.379
GL85	18.846	0.290	0.519	0.427
GL97	17.353	0.359	0.649	0.585
GM1	16.798	0.310	0.545	0.506
NL2	15.693	0.293	0.508	0.506

PNS is larger than that of an NS of the same mass [41].

The central baryon densities ρ_c of the PNS PSR J0737-3039A calculated with different nucleon coupling constants are different. ρ_c of the PNS PSR J0737-3039A calculated using GL97 is the largest, $\rho_c=0.359 \text{ fm}^{-3}$, whereas ρ_c calculated using DD-ME1 is the smallest, $\rho_c=0.247 \text{ fm}^{-3}$. That is, the central baryon density calculated using the five nucleon coupling constants is $\rho_c=0.247\text{--}0.359 \text{ fm}^{-3}$.

V. EFFECTIVE MASSES OF BARYONS AND THE CHEMICAL POTENTIALS OF NEUTRONS AND ELECTRONS

The effective mass of nucleons, Λ , Σ , and Ξ as a function of the baryon density ρ are shown in Fig. 2. We denote the center effective mass of nucleons, Λ , Σ , and Ξ as m_{Nc}^* , $m_{\Lambda c}^*$, $m_{\Sigma c}^*$, and $m_{\Xi c}^*$, respectively. As shown in Fig. 2, the effective masses of nucleons, Λ , Σ , and Ξ all decrease with increasing baryon density ρ . At the center of the PNS, the effective mass of the baryon reaches a minimum. Corresponding to the same baryon density ρ , the effective mass calculated using DD-ME1 is the smallest, whereas that calculated using GL97 is the largest. As shown in Table 2, the center effective masses of nucleons, Λ , Σ , and Ξ calculated using the above five groups of nucleon coupling constants are $m_{Nc}^*=384.521\text{--}606.324$

MeV, $m_{\Lambda c}^*=778.280\text{--}911.405 \text{ MeV}$, $m_{\Sigma c}^*=939.187\text{--}1080.822 \text{ MeV}$, and $m_{\Xi c}^*=1152.637\text{--}1218.964 \text{ MeV}$, respectively.

The chemical potentials of neutrons and electrons are shown in Fig. 3. The chemical potentials of neutrons μ_n and electrons μ_e increase with increasing baryon density ρ . Different nucleon coupling constants result in different chemical potentials relative to the same baryon density ρ . The central neutron chemical potential of the five nucleon coupling constants is calculated as $\mu_{nc}=5.340\text{--}5.516 \text{ fm}^{-1}$, and the central electron chemical potential is calculated as $\mu_{ec}=0.721\text{--}0.989 \text{ fm}^{-1}$.

VI. ENERGY DENSITY AND PRESSURE IN PNS PSR J0737-3039A

The energy density ε and pressure p in the PNS PSR J0737-3039A as a function of the baryon density ρ are shown in Fig. 4. Both the energy density ε and pressure p increase with increasing baryon density ρ . Corresponding to the same baryon density ρ , the energy densities calculated using different nucleon coupling constants have little difference; however, the calculated pressures differ greatly. The central energy density and central pressure calculated for the five sets of nucleon coupling constants are different. GL97 results in the maximum center energy density and center pressure.

As shown in Table 1, the minimum central energy

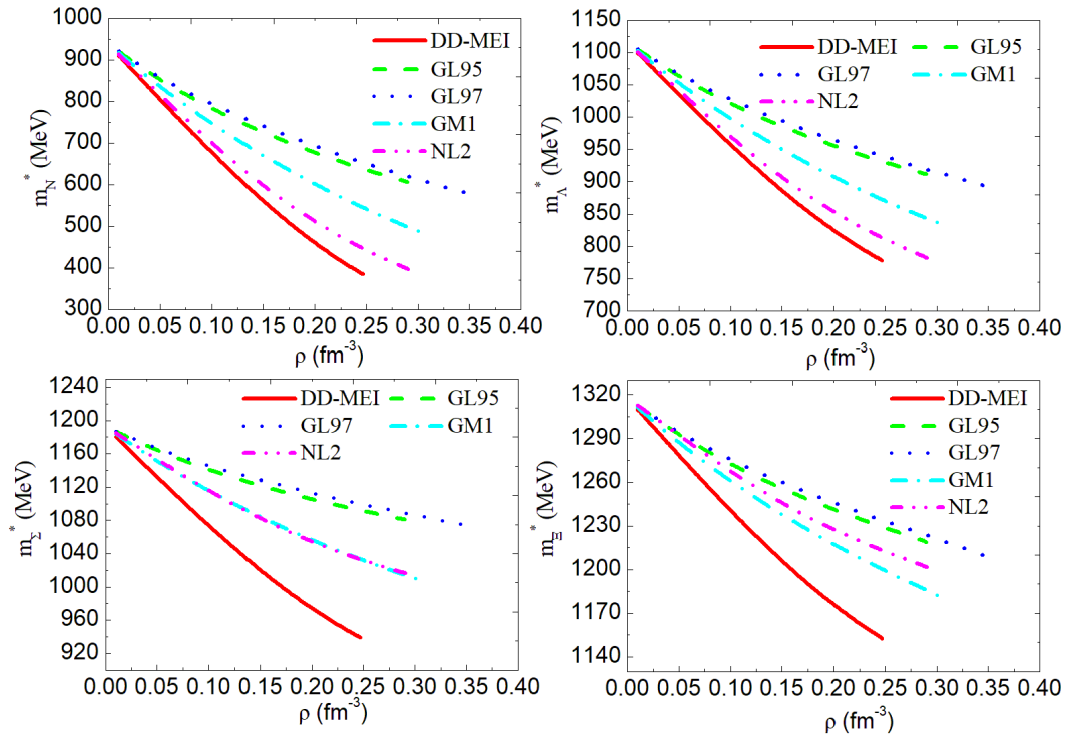


Fig. 2. (color online) Effective mass of baryons in the PNS PSR J0737-3039A as a function of baryon density. The five curves represent the results of the five nucleon coupling constants DD-ME1, GL85, GL97, GM1, and NL2.

Table 2. Effective mass of baryons and the chemical potentials of n and e in the PNS PSR J0737-3039A calculated in this study. $m_{N_c}^*$, $m_{\Lambda_c}^*$, $m_{\Sigma_c}^*$, and $m_{\Xi_c}^*$ are the center effective masses of nucleons N , Λ , Σ , and Ξ , respectively. μ_{nc} and μ_{ec} are central chemical potentials of n and e , respectively.

Parameter	$m_{N_c}^*/\text{MeV}$	$m_{\Lambda_c}^*/\text{MeV}$	$m_{\Sigma_c}^*/\text{MeV}$	$m_{\Xi_c}^*/\text{MeV}$	μ_{nc}/fm^{-1}	μ_{ec}/fm^{-1}
DD-ME1	384.521	778.280	939.187	1152.637	5.340	0.721
GL85	606.324	911.405	1080.822	1218.964	5.421	0.943
GL97	573.011	888.351	1071.635	1206.096	5.516	0.989
GM1	478.656	831.015	1006.070	1179.389	5.418	0.763
NL2	394.604	780.860	1015.662	1200.968	5.367	0.829

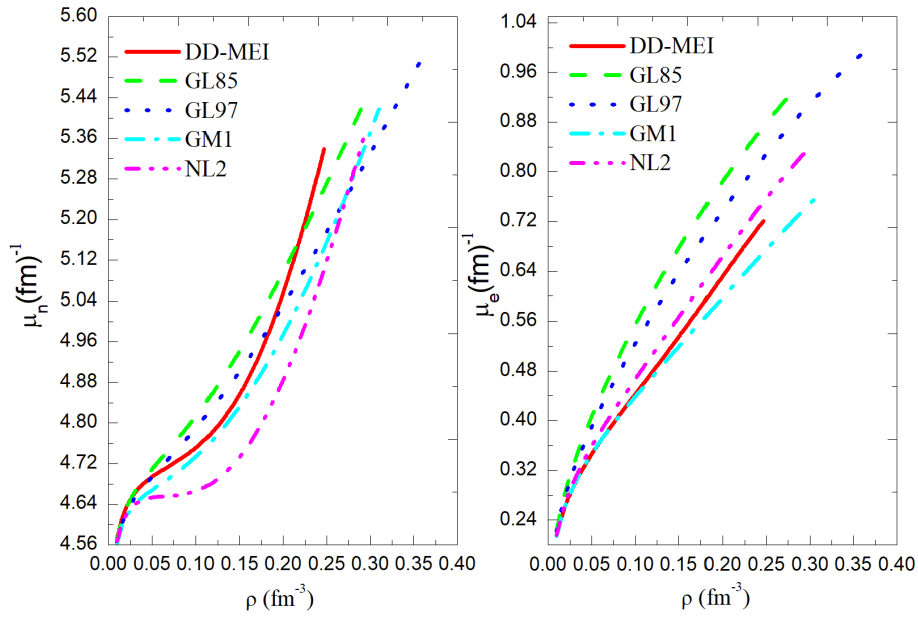


Fig. 3. (color online) Chemical potentials of neutrons and electrons in the PNS PSR J0737-3039A as a function of baryon density. The five curves represent the results of the five nucleon coupling constants DD-ME1, GL85, GL97, GM1, and NL2.

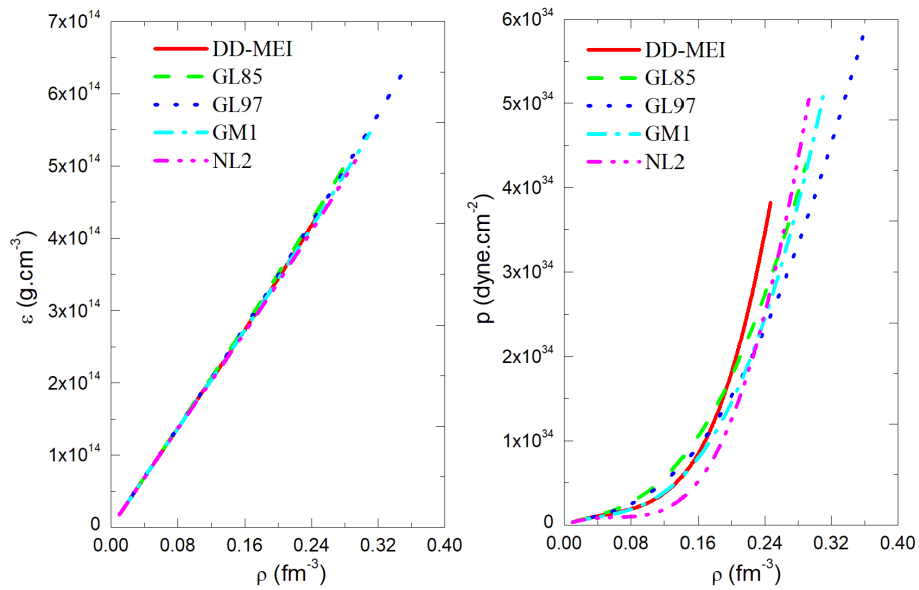


Fig. 4. (color online) Energy density and pressure in the PNS PSR J0737-3039A as a function of baryon density. The five curves represent the results of the five nucleon coupling constants DD-ME1, GL85, GL97, GM1, and NL2.

density given with DD-ME1 is $\varepsilon_c=4.30\times 10^{14}$ g·cm⁻³. GL97 gives the largest central energy density, $\varepsilon_c=6.49\times 10^{14}$ g·cm⁻³. The central energy density calculated from the five nucleon coupling constants is $\varepsilon_c=4.30\times 10^{14}$ – 6.49×10^{14} g·cm⁻³. Similarly, the central pressure calculated using the five nucleon coupling constants is $p_c=3.79\times 10^{34}$ – 5.85×10^{34} dyne·cm⁻².

VII. RELATIVE PARTICLE DENSITY IN PNS PSR J0737-3039A

Figure 5 shows the relative particle density ρ_i/ρ in the PNS PSR J0737-3039A as a function of the baryon density ρ .

As shown in Fig. 5 and Table 3, baryons n , p , Λ , Σ^+ , Σ^0 , Σ^- , Ξ^0 and Ξ^- all appear in the PNS PSR J0737-3039A when using the nucleon coupling constants DD-ME1, GL85, GL97, and GM1. However, with NL2, only baryons n , p , Λ , Σ^0 , Σ^- , Ξ^0 , and Ξ^- are present, while baryon Σ^+ is absent.

As shown in Fig. 5, corresponding to the same baryon density, the relative particle densities of the same baryon in the PNS PSR J0737-3039A calculated using dif-

ferent nucleon coupling constants differ greatly. As shown in Table 3, the central relative baryon densities of the PNS PSR J0737-3039A calculated using different nucleon coupling constants also differ greatly. For example, for hyperon Λ , the minimum central relative baryon density given using DD-ME1 is $\rho_{\Lambda c}/\rho=0.5\%$, whereas GL97 gives the largest central baryon density, $\rho_{\Lambda c}/\rho=2.8\%$. In other words, the central baryon density of the Λ -hyperon calculated using the five nucleon coupling constants is $\rho_{\Lambda c}/\rho=0.5\%$ – 2.8% . Similarly, the central baryon density of n calculated using five groups of nucleon coupling constants is $\rho_{nc}/\rho=80.5\%$ – 90.7% , the central baryon density of p is $\rho_{pc}/\rho=8.4\%$ – 17.5% , the central baryon density of the Σ^0 hyperon is $\rho_{\Sigma^0 c}/\rho=1.3\times 10^{-3}\%$ – $4.1\times 10^{-4}\%$, the central baryon density of the Σ^- hyperon is $\rho_{\Sigma^- c}/\rho=5.7\times 10^{-5}\%$ – 0.04% , the central baryon density of the Ξ^0 hyperon is $\rho_{\Xi^0 c}/\rho=1.5\times 10^{-5}\%$ – $2.4\times 10^{-3}\%$, and the central baryon density of the Ξ^- hyperon is $\rho_{\Xi^- c}/\rho=5.8\times 10^{-3}\%$ – 0.18% . The hyperon Σ^+ in the PNS PSR J0737-3039A calculated using NL2 does not appear, whereas the central baryon density of Σ^+ calculated using DD-ME1, GL85, GL97, and GM1 is $\rho_{\Sigma^+ c}/\rho=1.0\times 10^{-6}\%$ – $2.9\times 10^{-3}\%$.

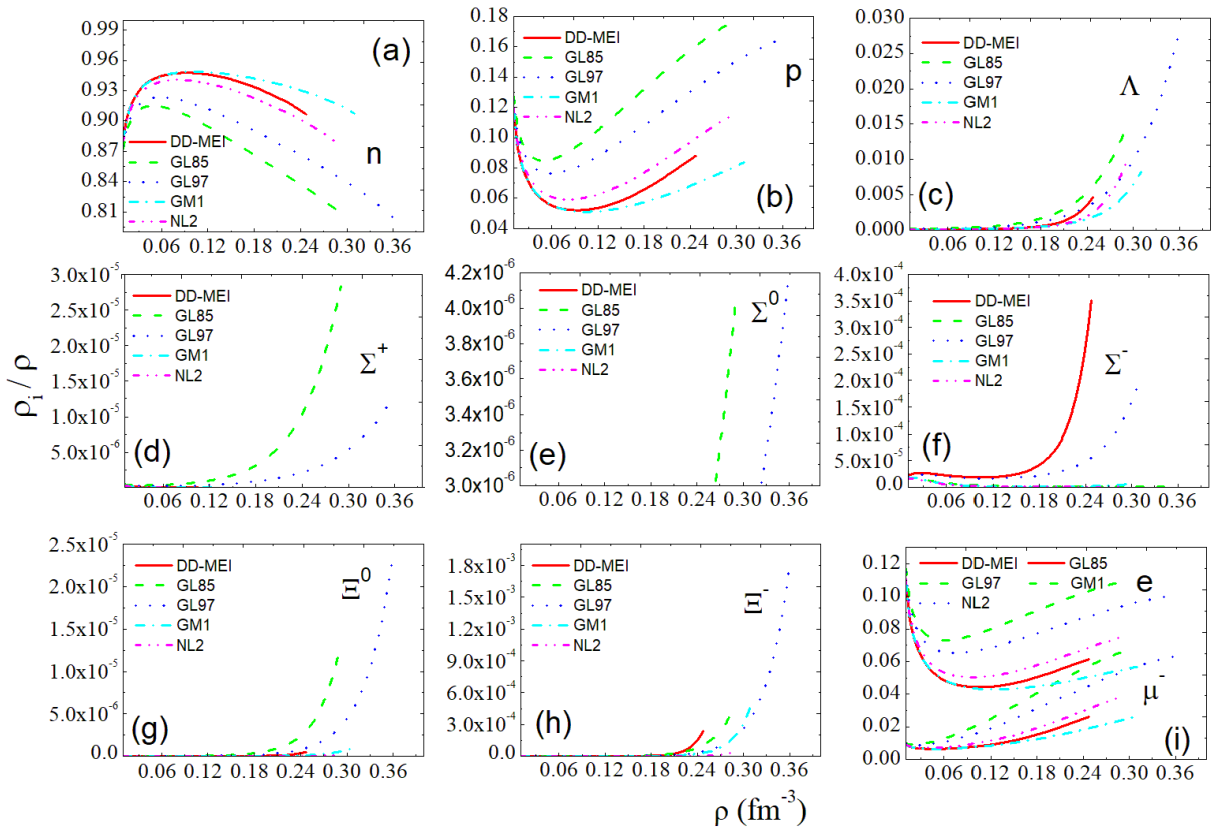


Fig. 5. (color online) Relative particle density in the PNS PSR J0737-3039A as a function of baryon density. The five curves represent the results of the five nucleon coupling constants DD-ME1, GL85, GL97, GM1, and NL2.

Table 3. Central relative particle densities in the PNS PSR J0737-3039A. ρ_{nc}/ρ , ρ_{pc}/ρ , $\rho_{\Lambda c}/\rho$, $\rho_{\Sigma^+ c}/\rho$, $\rho_{\Sigma^0 c}/\rho$, $\rho_{\Sigma^- c}/\rho$, $\rho_{\Xi^0 c}/\rho$, and $\rho_{\Xi^- c}/\rho$ are the central relative particle densities of n , p , Λ , Σ^+ , Σ^0 , Σ^- , Ξ^0 , and Ξ^- , respectively, in the PNS PSR J0737-3039A.

Parameter	ρ_{nc}/ρ %	ρ_{pc}/ρ %	$\rho_{\Lambda c}/\rho$ %	$\rho_{\Sigma^+ c}/\rho$ %	$\rho_{\Sigma^0 c}/\rho$ %	$\rho_{\Sigma^- c}/\rho$ %	$\rho_{\Xi^0 c}/\rho$ %	$\rho_{\Xi^- c}/\rho$ %
DD-ME1	90.7	8.8	0.5	1E-6	2.0E-4	0.04	5.1E-5	0.02
GL85	81.0	17.5	1.5	2.9E-3	4.0E-4	5.7E-5	1.3E-3	0.05
GL97	80.5	16.5	2.8	1.3E-3	4.1E-4	1.3E-4	2.4E-3	0.18
GM1	90.7	8.4	0.8	2E-6	1.8E-4	0.02	1.07E-4	0.05
NL2	87.5	11.5	1.0	0	1.3E-5	5.2E-4	1.5E-5	5.8E-3

VIII. SUMMARY

In this study, the influence of nucleon coupling constants on the properties of the PNS PSR J0737-3039A is investigated using RMF theory. Here, five sets of nucleon coupling constants (DD-ME1, GL85, GL97, GM1, and NL2) are used, and the temperature of the PNS PSR J0737-3039A is chosen as $T=20$ MeV.

The radius R , central baryon density ρ_c , central energy density ε_c , and central pressure p_c of the PNS PSR J0737-3039A calculated using different nucleon coupling constants are different. Using these five sets of nucleon coupling constants, we find that the radius of the PNS PSR J0737-3039A is $R=15.693-18.846$ km, the central baryon density is $\rho_c=0.247-0.359$ fm $^{-3}$, the central energy density is $\varepsilon_c=4.30\times 10^{14}-6.49\times 10^{14}$ g \cdot cm $^{-3}$, and the central pressure is $p_c=3.79\times 10^{34}-5.85\times 10^{34}$ dyne \cdot cm $^{-2}$. Although the PNS radius should be larger than that of an NS of the same mass, it should not be significantly larger. As shown in Table 1, the radius of the PNS PSR J0737-3039A calculated using the nucleon coupling constant NL2 is the smallest, $R=15.693$ km, and is closest to the radius calculated by Riley *et al.* and Miller *et al.* Therefore, NL2 seems to be the most reasonable coupling constant.

For four sets of nucleon coupling constants (DD-ME1, GL85, GL97 and GM1), baryons n , p , Λ , Σ^+ , Σ^0 , Σ^- , Ξ^0 , and Ξ^- all appear in the PNS PSR J0737-3039A. However, using NL2, only baryons n , p , Λ , Σ^0 , Σ^- , Ξ^0 , and Ξ^- are present, while baryon Σ^+ does not appear.

Corresponding to the same baryon density, the relative densities of the same baryon in the PNS PSR J0737-3039A calculated using different nucleon coupling constants differ greatly. The central relative baryon densities of the PNS PSR J0737-3039A calculated using different nucleon coupling constants also differ greatly. The central baryon density of n calculated using the five groups of nucleon coupling constants is $\rho_{nc}/\rho=80.5\%-90.7\%$, the central baryon density of p is $\rho_{pc}/\rho=8.4\%-17.5\%$, the central baryon density of Λ is $\rho_{\Lambda c}/\rho=0.5\%-2.8\%$, the central baryon density of the Σ^0 hyperon is $\rho_{\Sigma^0 c}/\rho=1.3\times 10^{-3}\%-4.1\times 10^{-4}\%$, the central baryon density of the Σ^- hyperon is $\rho_{\Sigma^- c}/\rho=5.7\times 10^{-5}\%-0.04\%$, the central baryon density of the Ξ^0 hyperon is $\rho_{\Xi^0 c}/\rho=1.5\times 10^{-5}\%-2.4\times 10^{-3}\%$, and the central baryon density of the Ξ^- hyperons is $\rho_{\Xi^- c}/\rho=5.8\times 10^{-3}\%-0.18\%$. The hyperon Σ^+ does not appear with NL2, whereas the central baryon density of hyperon Σ^+ calculated using DD-ME1, GL85, GL97, and GM1 is $\rho_{\Sigma^+ c}/\rho=1.0\times 10^{-6}\%-2.9\times 10^{-3}\%$.

References

- [1] A. G. Lyne, M. Burgay, and M. Kramer *et al.*, *Science* **303**, 1153 (2004)
- [2] Z. L. Deng, Z. F. Gao, X. D. Li *et al.*, *ApJ* **892**, 4 (2020)
- [3] S. E. Thorsett and D. Chakrabarty, *ApJ* **512**, 288 (1999)
- [4] M. Bailes, S. M. Ord, and H. S. Knight *et al.*, *ApJ* **595**, L49 (2003)
- [5] I. A. Morrison, T. W. Baumgarte, and S. L. Shapiro *et al.*, *ApJ* **617**, L135-L138 (2004)
- [6] M. Kramer, I. H. Stairs, and R. N. Manchester *et al.*, *Science* **314**, 97-102 (2006)
- [7] A. Worley, P. G. Krastev, and B. A. Li, *ApJ* **685**, 390-399 (2008)
- [8] P. Landry and B. Kumar, *ApJL* **868**, L22 (2018)
- [9] N. A. Avdeev, P. I. Dyadina, and S. P. Labazova, *J Exp. Theor. Phys.* **131**, 537-547 (2020)
- [10] D. H. Wen, W. Chen, Y. G. Lu *et al.*, *Mod. Phys. Lett. A* **22**, 631 (2007)
- [11] H. Y. Jia, B. X. Sun, J. Meng *et al.*, *Chin. Phys. Lett.* **18**, 1571 (2001)
- [12] C. Zhu, Z. F. Gao *et al.*, *Mod. Phys. Lett. A* **31**, 1650070 (2016)
- [13] Y. Lim, A. Bhattacharya, J. W. Holt *et al.*, *Phys. Rev. C* **104**, L032802 (2021)
- [14] P. C. Chu, Y. Zhou, Y. Y. Jiang *et al.*, *Eur. Phys. J. C* **81**, 93 (2021)
- [15] Z. F. Gao, H. Shan, and H. Wang, *Astron. Nachr.* **342**, 369-376 (2021)
- [16] H. Wang, Z. F. Gao, H. Y. Jia *et al.*, *Universe* **6**, 63 (2020)
- [17] P. B. Demorest, T. Pennucci, S. M. Ransom *et al.*, *Nature* **467**, 1081 (2010)
- [18] E. Fonseca, T. T. Pennucci, J. A. Ellis *et al.*, *ApJ* **832**, 167 (2016)
- [19] J. Antoniadis, P. C. C. Freire, N. Wex *et al.*, *Science* **340**, 448 (2013)
- [20] H. T. Cromartie, E. Fonseca, S.M. Ransom *et al.*, *Nat. Astron.* **4**, 72 (2020)

- [21] A. Burrows and J. M. Lattier, *Astrophys.* **307**, 178 (1986)
- [22] S. G. Zhou, *Phys. Scripta* **91**, 063008 (2016)
- [23] J. Schaffner, C. B. Dover, and A. Gal, *Ann. Phys.* **235**, 35 (1994)
- [24] N. K. Glendenning, *Compact Stars: Nuclear Physics, Particle Physics, and General Relativity*, Springer-Verlag, New York, Inc, 1997
- [25] N. K. Glendenning, *Phys. Lett. B* **185**, 275 (1987)
- [26] N. K. Glendenning, *Nucl. Phys. A* **469**, 600 (1987)
- [27] R. C. Tolman, *Phys. Rev.* **55**, 364 (1939)
- [28] J. R. Oppenheimer and G. M. Volkoff, *Phys. Rev.* **55**, 374 (1939)
- [29] S. Typel and H. H. Wolter, *Nucl. Phys. A* **656**, 331 (1999)
- [30] N. K. Glendenning, *ApJ* **293**, 470 (1985)
- [31] N. K. Glendenning and S. A. Moszkowski, *Phys. Rev. Lett.* **67**, 2414 (1991)
- [32] S. J. Lee *et al.*, *Phys. Rev. Lett.* **57**, 2916 (1986)
- [33] J. Schaffner and I. N. Mishustin, *Phys. Rev. C* **53**, 1416 (1996)
- [34] J. Schaffner-Bielich and A. Gal, *Phys. Rev. C* **62**, 034311 (2000)
- [35] S. Weissenborn, D. Chatterjee, and J. Schaffner-Bielich, *Nucl. Phys. A* **881**, 62 (2012)
- [36] A. Gal, E. V. Hungerford, and D. J. Millener, *Rev. Mod. Phys.* **88**, 035004 (2016)
- [37] C. J. Batty, E. Friedman, and A. Gal, *Phys. Rep.* **287**, 385 (1997)
- [38] T. Harada, Y. Hirabayashi, and A. Umeya, *Phys. Lett. B* **690**, 363 (2010)
- [39] T. E. Riley, A. L. Watts, S. Bogdanov *et al.*, *ApJL* **887**, L21 (2019)
- [40] M. C. Miller, F. K. Lamb, A. J. Dittmann *et al.*, *ApJL* **887**, L24 (2019)
- [41] X. F. Zhao, *Astrophys. Space Sci.* **362**, 95 (2017)